We are IntechOpen,
the world's leading publisher of
Open Access books
Built by scientists, for scientists

6,000
Open access books available

148,000
International authors and editors

185M
Downloads

Our authors are among the

154
Countries delivered to

TOP 1%
most cited scientists

12.2%
Contributors from top 500 universities

BOOK CITATION INDEX
CLARIVATE ANALYTICS
INDEXED

WEB OF SCIENCE™

Selection of our books indexed in the Book Citation Index
in Web of Science™ Core Collection (BKCI)

Interested in publishing with us?
Contact book.department@intechopen.com

Numbers displayed above are based on latest data collected.
For more information visit www.intechopen.com

Chapter

Design Optimization of 18-Poled High-Speed Permanent Magnet Synchronous Generator

Aslan Deniz Karaoglan, Deniz Perin and Kemal Yilmaz

Abstract

The aim of this research is to optimize the design of an 18-poled 8000 rpm 7 kVA high-speed permanent magnet synchronous generator. The goal is to find the best factor levels for the design parameters, namely magnet thickness (MH), offset, and embrace (EMB) to optimize the responses namely efficiency (%), rated torque (N.m), air-gap flux density (Tesla), armature current density (A/mm^2), armature thermal load (A^2/mm^3). The aim is to keep the air-gap flux density at 1 tesla while maximizing efficiency and minimizing the rest of the responses. Optimization was carried out with one sample algorithm selected from each of the commonly used optimization algorithm classifications. For this purpose, different class of well-known optimization techniques such as response surface methodology (gradient-based methods), genetic algorithm (evolutionary-based algorithms), particle swarm optimization algorithm (swarm-based optimization algorithms), and modified social group optimization algorithm (human-based optimization algorithms) are selected. In the Ansys Maxwell environment, numerical simulations are carried out. Mathematical modeling and optimizations are performed by using Minitab and Matlab, respectively. Confirmations are also performed. Results of the comparisons show that modified social group optimization and particle swarm optimization algorithms a bit outperform the response surface methodology and genetic algorithm, for this design problem.

Keywords: high-speed alternator, permanent magnet synchronous generator, electric machine design, design optimization, response surface methodology, modified social group optimization algorithm, particle swarm optimization algorithm, genetic algorithm

1. Introduction

Many researchers have studied magnetic device design optimization and permanent magnet synchronous generator (PMSG) design optimization, which are investigated in many research studies over the last few decades. Efficiency, magnetic flux density distribution, total harmonic distortion (THD), and other performance criteria are commonly used in these studies and are attempted to be improved [1–11]. The most common problems are heat buildup in the rotor, balancing issues, and bearing

issues. Magnetic flux density distribution is a key success criterion that must be maintained within a specific range in order to provide high efficiency and low heating for the electric machine. Many different methods are used for design optimization. It is impossible to perform optimization using real experimental results because there are so many design combinations. In most cases, simulation results are used instead. However, there are limited numbers of studies about high-speed alternator design optimization.

Sadeghierad et al. [12] studied on performance comparisons of alternative designs of high-speed alternators (HSA) for microturbines and considered the design difficulties. Sadeghierad et al. [13] studied on optimizing the design of a high-speed axial flux generator (HSAFG) by the aid of particle swarm optimization (PSO) and genetic algorithm (GA) to maximize the efficiency. They discussed the effect of the lambda, which is the ratio of inner diameter to outer diameter. Ismagilov et al. [14] tested a new topology of the stator magnetic core made of amorphous alloy for a 5 kW 60,000 rpm high-speed permanent magnet electric machine with a tooth-coil winding with six slots and two and four poles. Guo et al. [15] presented a method for determining the back electromotive force (EMF) utilizing air gap static flux density distribution and calculating the coil average inductance at the midline of the quadrature-direct axis. They used gradient descent-based optimization to minimize the volume of high-speed generator for micro turbojet engine. The summary for the state of the art is given in **Table 1**.

As can be seen from the literature review, the studies about design optimization of high-speed generator by using optimization methods are very limited. Also the results those presented to show the performance comparisons of the meta-heuristic optimization methods are very poor.

The motivation of this study is to perform design optimization of 18-Poled 8000 rpm 7 kVA high-speed PMSG. This problem is important because of the high rotor speed and high frequency of the stator flux variation; the design of a high-speed machine differs significantly from the design of a conventional machine with low speed and low frequency. The first motivation of this study is to contribute to the knowledge that has emerged based on the limited number of studies on this subject in the literature, with a new study on topology optimization of high-speed PMSGs.

The second motivation is to show the performance of the different class of optimization techniques on the design problem of high-speed alternators to the related researchers. Deterministic or stochastic algorithms can be used for optimization. Due to their high processing demands, deterministic approaches are ineffective for handling multimodal and nonlinear complex issues. The nature is a major source of inspiration for meta-heuristic algorithms, which are stochastic approaches utilized for

Author(s)	Year	Subject	Optimization method
Sadeghierad et al.	2006	HSA for microturbines	N/A
Sadeghierad et al.	2010	HSAFG	PSO, GA
Ismagilov et al.	2018	5 kW 60,000 rpm high-speed permanent magnet electric machine	N/A
Guo et al.	2019	High speed generator for micro turbojet engine	Gradient descent method

Table 1.
Summary of the literature review.

2

optimization. There are four different types of meta-heuristics: (*i*) evolutionary, (*ii*) swarm, (*iii*) physical and chemical, and (*iv*) human. Various well-known optimization methods, such as response surface methodology (RSM) (gradient-based methods), GA (evolutionary-based algorithms), PSO (swarm-based optimization algorithms), and modified social group optimization algorithm (MSGO) (human-based optimization algorithms), are used for this purpose.

The selected design parameters (magnet thickness (MH), offset, embrace (EMB)) and the responses (efficiency (%), rated torque (N.m), air-gap flux density (Tesla), armature current density (A/mm^2), armature thermal load (A^2/mm^3)) are not previously used together for high-speed alternator design optimization problem. So this is the novelty aspect of this research.

This research was carried out in a real industrial plant, and by focusing on a small number of parameters, we hoped to have a smaller impact on the layout and operation of a serial production line (Such as redesigning assembly parts that may have an impact on standard production, cooling design, body design, and so on.). As a result, the parameters (magnet thickness (MH), offset, embrace (EMB)) that have the least impact on the outer dimensions of the alternator are chosen as the design parameters (factors). The following section goes over the materials and methods.

2. Materials and methods

2.1 Regression modeling and response surface methodology (RSM)

The design optimization problem that is handled in this study is solved in three steps: *i*) design the experiments and perform the experimental runs, *ii*) perform regression modeling to determine the mathematical relations between the responses and the factors, *iii*) perform optimization to determine the optimum factor levels. The goal of this paper is to calculate the optimum levels of magnet thickness (X_1), offset (X_2), and embrace (X_3) to maximize the efficiency and to minimize the rated torque, armature current density, and armature thermal load, while keeping the air-gap flux density at 1.0 Tesla. Linear, quadratic, and interaction terms can all be found in regression models. These three terms occur simultaneously in a full quadratic model. Eq. (1) provides the full quadratic model's general representation [16–18].

$$Y_i = \beta_0 + \sum_{k=1}^{m} \beta_k X_{ki} + \sum_{k=1}^{m} \beta_{kk} X_{ki}^2 + \sum_{k<l}^{m} \beta_{kl} X_{ki} X_{li} + e_i \tag{1}$$

$$\boldsymbol{\beta}^T = [\beta_0, \beta_1, \beta_2, \dots, \beta_m] \tag{2}$$

The response value for the ith experimental run is represented by Y_i. In this study, five different regression equations—which belong to five responses—will be calculated in the next section. X_{ki} and X_{ki}^2 terms are the linear and quadratic terms, respectively, while $X_{ki} X_{li}$ terms represent the interactions ($X_1 X_2$, $X_1 X_3$, $X_2 X_3$). Finally, e_i is the residual error. The vector given in Eq. (2) contains the model's coefficients given in Eq. (1) and calculated as shown below [16–18]:

$$\beta = \left(X^T X\right)^{-1} \left(X^T Y\right) \tag{3}$$

Y is referred to as the response, and it is denoted by a column vector. In this study, the response values are obtained using Maxwell simulations. **X** is a matrix, and it is made up of the various combinations of the design parameters involved in the experimental design. The first column of the X is made up of 1 s for the model's constant term (β_0). The second, third, and fourth columns contain the factor values X_1, X_2, and X_3, respectively. The experiments in this study are divided into 14 runs. These three columns (the second, third, and fourth columns) and 14 rows are identical to the experimental design. The squares of X_1, X_2, and X_3 make up the 5th, 6th, and 7th columns of the **X** matrix, respectively. The same issue applies to interactions. By multiplying the related columns of X_1, X_2, and X_3, the interactions are placed in the 8th, 9th, and 10th columns of the **X** matrix.

After mathematical modeling, R^2 (coefficient of determination) is calculated to determine whether the factors are sufficient to describe the response change. To put it another way, R^2—which is presented in Eq. (4)—represents the level of explanatory power between the regression model and the factors.

$$R^2 = \frac{\beta^T X^T Y - n\bar{Y}^2}{Y^T Y - n\bar{Y}^2} \tag{4}$$

In order to use these models established in Eq. (1)–(3) during the optimization phase, R^2 must be closer to 1 (which means 100%). Then this means the factors of the mathematical models are sufficient to explain the shifts at Y, and in this case this means there is no need to add new factors to the regression model. The significance of the models must be determined in the final step before optimization. This is done using analysis of variance (ANOVA). The F-test is used in ANOVA to test the significance of a regression model. In this study, we used "p-value" technique (where the p-values of the each model are calculated using Minitab statistical analysis program). When the p-value is less than the alpha (type-I error), the model is considered significant. We set confidence level at 95% in the statistical analysis. This indicates that the type-I error==0.05 (5%).

In the second phase, the optimization algorithms will be run through these five regression models to calculate the optimum factor levels. In this study, four different classes of optimization methods (RSM, GA, PSO, and MSGO) are tried on this optimization problem. RSM is a gradient-based deterministic optimization method; however, GA, PSO, and MSGO are the meta-heuristics. Meta-heuristic algorithms can be classified into different groups such as evolutionary, swarm-based, human-based, etc.

Since its introduction in 1951, the RSM has become a commonly preferred design of experiment (DOE) approach for modeling and optimizing processes with a small number of experimental runs [16–18]. In this study, RSM is applied by using "Minitab Response optimizer Module," which uses gradient search algorithm in its background.

2.2 Genetic algorithm (GA)

Meta-heuristic algorithms are stochastic optimization methods that are heavily influenced by nature. In 1975, Holand created GA, a search and optimization technique [18]. Natural selection and genetic concepts are used to replicate the evolutionary process in nature. It operates based on probability laws and simply requires the purpose function. The solution area is partially investigated by GA, resulting in a more efficient search in a shorter amount of time. Chromosomes are created in the initial

phase of GA to explore potential solutions. Chromosome set represents the generation's population. Selection, crossover, and mutation are the three GA operators. These operators drive the evolution of chromosomes in a generation toward the following generation. There are several uses for GA, including scheduling, vehicle routing, and transportation. GA is an evolutionary-based algorithm [19, 20]. According to Haupt and Haupt [21], since the chromosomes are not decoded before calculating the cost function, continuous GA is faster than binary GA. As a result, instead of binary GA, continuous GA was used in this study because it has the advantage of requiring less storage. In this study, the crossing method, in which Haupt & Haupt [19] combine the extrapolation method with a crossing method, is used.

2.3 Particle swarm optimization (PSO) algorithm

Particle swarm optimization (PSO) algorithm is invented by Kennedy & Eberhart [22] in 1995, and it is the first swarm-based meta-heuristic algorithm. Every possible solution in PSO is represented by a particle. The distances between a particle's present position and its best position and the best position of the group are used in PSO to update a particle's velocity [23–25].

The velocity vector and position vector for the ith particle are shown by v_i and x_i, respectively, in the D-dimensional search space (where $v_i = (v_{i1}, v_{i2}, \ldots, v_{iD})$ and $x_i = (x_{i1}, x_{i2}, \ldots, x_{iD})$). After random initialization of particles, each particle's velocity and position are updated as specified in Eq. (5) and Eq. (6) [25].

$$v_i(t+1) = wv_i(t) + c_1r_1\big(p_i - x_i(t)\big) + c_2r_2\Big(p_g - x_i(t)\Big) \tag{5}$$

$$x_i(t+1) = x_i(t) + v_i(t+1) \tag{6}$$

In these equations, w stands for the inertia weight and is used to regulate how the previous velocity affects the new. The best past positions of the ith individual and all particles in the current generation are represented, respectively, by p_i and p_g. The constants c_1 and c_2 are used to weight the positions. The uniformly distributed values between $[0, 1]$ are $[r_1]$ and $[r_2]$. **Figure 1** shows the algorithm's progress [25].

2.4 The modified social group optimization (MSGO) algorithm

MSGO is a human-based optimization algorithm and invented in 2020. It is proposed by Naik et al. [26] by improving the acquiring phase of social group optimization (SGO) algorithm [27] and introducing a self-awareness probability factor. It is based on an individual's social behavior in a group to solve complex problems.

In MSGO, each member of the group (person) stands in for a potential solution, and the human traits—which stand in for a person's dimension—represent the amount of design variables in the issue. **Figure 2** below shows the pseudocode for the improvement phase. In **Figure 2**, P_i represents the members of the social group made up of N individuals, where $i = 1,2,3,\ldots,N$. Each individual additionally has D traits $(P_i = (P_{i1}, P_{i2}, \ldots, P_{iD}))$. The self-introspection parameter between $[0,1]$ and *rand* $\sim U(0, 1)$ is called c. The best member of the group is *gbest*, who works to spread knowledge among all people. *Gbest* will then be able to assist the group as a whole in learning more. Eq. (7) presents the aim as a minimization problem. **Figure 2** and Eq. (7) illustrate the update for each individual [26, 27].
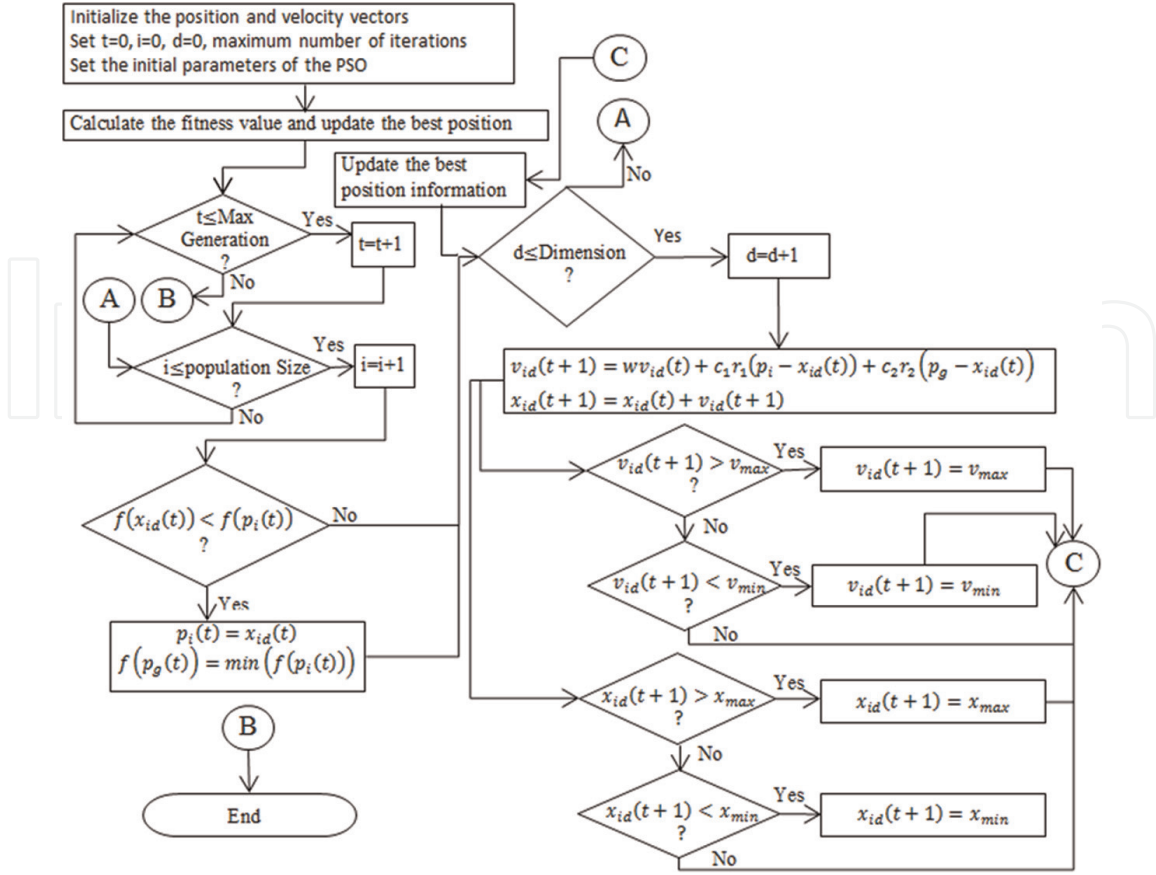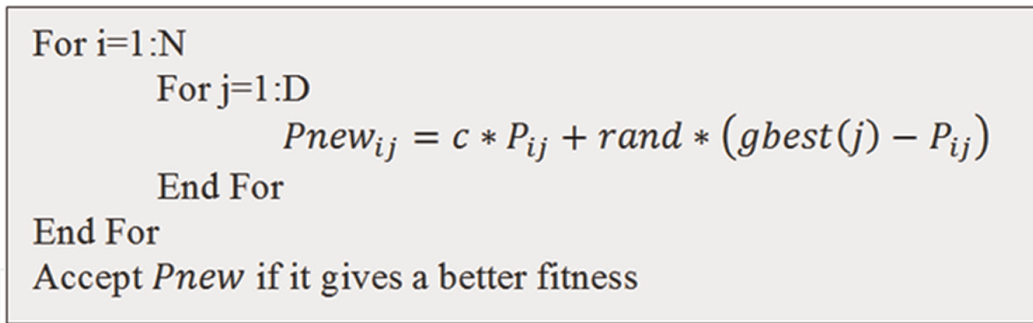
Figure 1.
The PSO algorithm.

Figure 2.
The improving phase.

$$[minvalue, index] = min\{f(P_i), i = 1, 2, ..., N\} and gbest = P(index, :)$$ (7)

A person interacts with the group's best member (*gbest*) as well as other group members at random during the learning phase in order to gain information. In other terms, gbest is the best member of the group. A person learns something new if someone else is more knowledgeable. The person with the most knowledge, or "gbest," has the most influence over others to learn from. Even if they are more knowledgeable than they are, group members can teach a person something new. The acquiring phase is represented by Eq. (8) and **Figure 3** [26, 27].

$$[minvalue, index] = min\{f(P_i), i = 1, 2, ..., N\} and gbest = P(index, :)$$ (8)

```
For i=1:N
Select randomly a person Pr (where i ≠ r)
    If f(Pi) < f(Pr)
        For j=1:D
            Pnewij = Pij + rand1 * (Pij − Prj)+rand2 * (gbest(j) − Pij)
        End For
    Else
        For j=1:D
            Pnewi,: = Pi,: + rand1 * (Pr,: − Pi,:)+rand2 * (gbest(j) − Pij)
        End For
    End If
Accept Pnew if it gives a better fitness than P
End For
```

Figure 3.
The acquiring phase for SGO.

```
For i=1:N
Select randomly a person Pr (where i ≠ r)
    If f(Pi) < f(Pr)
        If rand > SAP
            For j=1:D
                Pnewij = Pij + rand1 * (Pij − Prj)+rand2 * (bestP(j) − Pij)
            End For
        Else
            For j=1:D
                Pnewi,: = lb + rand * (ub − lb)
            End For
        End If
    Else
        For j=1:D
            Pnewij = Pij + rand1 * (Prj − Pij)+rand2 * (bestP(j) − Pij)
        End For
    End If
Accept Pnew if it gives a better fitness than P
End For
```

Figure 4.
The acquiring phase for MSGO.

where the updated values at the conclusion of the improving phase are P_i values.

By changing the acquisition step of the SGO algorithm, the MSGO algorithm was created. The improving phase, however, is identical to SGO. Each social group member is still interacting with the finest individual throughout this period ($best_p$). Each person also engages in interaction with the other group members to learn. During this stage, if the other person knows more, the person learns something new. If one person knows more than another and that person has a greater self-awareness probability (SAP) of learning that knowledge, then that person learns something new from that other person. SAP is the capacity to learn from others, according to its definition. Modified acquisition phase is shown in Eq. (9), and **Figure 4** below shows a minimization problem [26, 27]:

$$[\text{value, index\_num}] = \min\{f(P_i), i = 1, 2, \ldots, N\} \text{ and } best_P = P(\text{index\_num}, :)$$

$$\tag{9}$$

The relevant design variable's upper and lower bounds are shown in **Figure 4** as lb and ub, respectively. It is proposed to select the SAP between: $0.6 \leq SAP \leq 0.9$. According to the literature, MSGO shows best performance for SAP = 0.7 and c = 0.2 [26, 27].

3. Experimental results and discussions

We used an 18-poled 8000 rpm 7 kVA PMSG in this study. The design is done using Maxwell. **Table 2** lists the design parameters. The PMSG's structure is also shown in **Figure 5**. The rated power factor of the PMSG is 1.0. All of the winding material in the Maxwell design is standard copper. Lamination is done with Si-Fe. Finally, the insulation material H-Class is chosen.

The goal of the first stage is to use regression modeling to find the mathematical relationship between the factors (magnet thickness (X_1), offset (X_2), and embrace (X_3)) and the responses (efficiency (%), rated torque (N.m), air-gap flux density (Tesla), armature current density (A/mm^2), armature thermal load (A^2/mm^3)) by using regression modeling. "RSM face-centered design" is used to create an experiment to complete this phase. The factor levels for this experimental design are shown in **Table 3**. **Figure 6** shows a graphical representation of the experimental design. The level-2 for embrace in a standard face-centered design is 0.8%. However, due to the restrictions of the serially configured production line, we used 0.8% in the experimental design instead of 0.75%.

According to the graphical representation of experimental design that is presented in **Figure 6**, it can be clearly indicated that there are 15 experimental runs for three factors. However, no simulation could be made in Ansys Maxwell for the $(-1, +1, +1)$

Name	Value	Unit	Part	Description
Machine type	N/A	—	—	3-phase adjust speed PMSG
Inner dia.	100	Mm	Stator	Gap side core diameter
Outer dia.	160	Mm	Stator	Yoke side core diameter
Length	50	Mm	Stator	Length of the core
Skew width	1	Units	Stator	Slot range number
Slot type	3	N/A	Stator	Circular
Slots	54	Units	Stator	Number of slots
Bs1	2.7	Mm	Stator	Tooth width
Hs0	0.5	Mm	Stator	Slot opening height
Hs2	23	Mm	Stator	Slot height
Inner dia.	30	Mm	Rotor	Gap side core diameter
Outer dia.	99	Mm	Rotor	Yoke side core diameter
Length	50	Mm	Rotor	Length of the core
Poles	18	—	Rotor	Number of poles
Magnet	NdFe35	—	Rotor	Magnet type

Table 2.
Design parameters of 18-poled 8000 rpm 7 kVA PMSG.
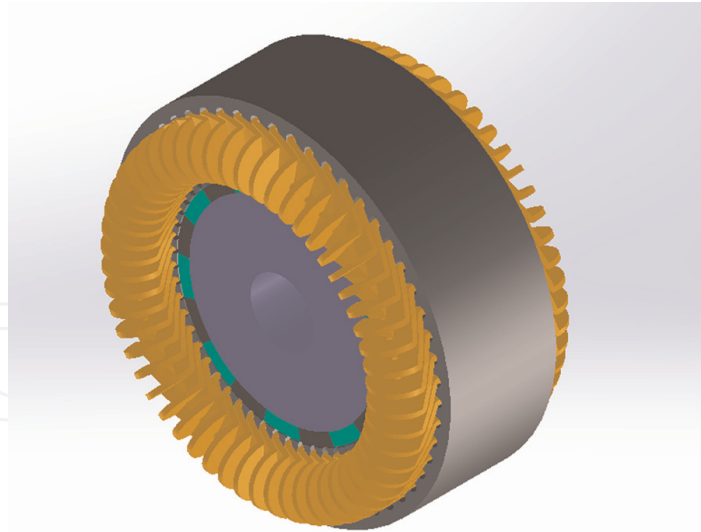
Figure 5.
Structure of the PMSG.

Factors	Symbols	Unit	Levels		
			−1	**0**	**1**
Magnet thickness	X_1	mm	2	4	6
Offset	X_2	mm	0	20	40
Embrace	X_3	%	0.5	0.8	1

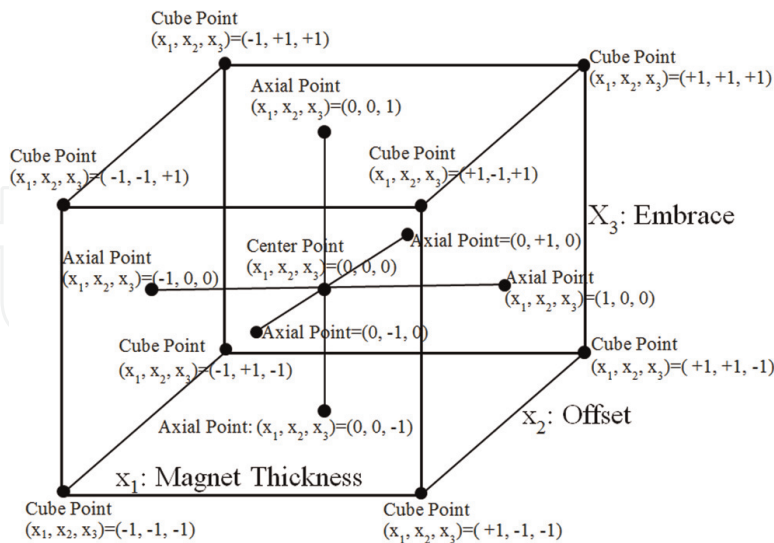**Table 3.**
Levels of factors.

Figure 6.
Graphical representation of RSM face-centered design.

experiment (magnet thickness: 2 mm, offset: 40 mm, embrace: 1%) in this experimental design. It is not a suitable design because the offset magnet is much larger than the thickness. Therefore, since such a magnet cannot be produced, this simulation does not yield results. At the end of Maxwell simulation, it gives an error "ARC Offset is too big." The findings of 14 experimental runs using Maxwell simulations are

Run	Factors						Responses				
i	Uncoded			Coded			Efficiency (%)	Rated Torque (N.m)	Air-Gap Flux Density (T)	Armature Current Density (A/mm²)	Armature Thermal Load (A²/mm³)
	X_{i1}	X_{i2}	X_{i3}	X_{i1}	X_{i2}	X_{i3}	Y_{i1}	Y_{i2}	Y_{i3}	Y_{i4}	Y_{i5}
1	2	0	0.5	−1	−1	−1	94.08	8.88	0.89	9.86	726.16
2	6	0	0.5	1	−1	−1	93.36	8.95	1.01	10.50	822.86
3	2	40	0.5	−1	1	−1	92.58	9.02	0.89	11.17	931.11
4	6	40	0.5	1	1	−1	92.21	9.06	1.02	11.80	982.58
5	2	0	1	−1	−1	1	97.54	8.56	0.89	6.11	278.45
6	6	0	1	1	−1	1	98.02	8.52	1.02	5.42	219.37
7	6	40	1	1	1	1	94.69	8.82	1.02	9.30	645.47
8	2	20	0.8	-1	0	0	96.61	8.64	0.89	7.28	396.00
9	6	20	0.8	1	0	0	97.00	8.61	1.02	6.78	343.20
10	4	0	0.8	0	−1	0	97.46	8.57	0.99	6.22	288.41
11	4	40	0.8	0	1	0	95.01	8.79	0.99	8.99	602.48
12	4	20	0.5	0	0	-1	93.61	8.92	0.99	10.29	789.81
13	4	20	1	0	0	1	97.53	8.57	0.99	6.13	280.17
14	4	20	0.8	0	0	0	97.07	8.61	0.99	6.72	336.90

Table 4.
Ansys Maxwell simulation results.

presented in **Table 4**. The disadvantage of making genuine PMSG prototypes—which is unpredictable due to expenses—is avoided in this approach. The original uncoded factor levels are also coded by using Eq. (10) given below. The mathematical modeling will be performed in terms of both uncoded and coded factor levels. Mathematical models for uncoded factor levels display the real relationship to the readers, while the models for coded factor levels will be used in the optimization phase (the details of which will be expanded in the following paragraphs).

$$X_{coded} = \frac{X_{uncoded} - ((X_{max} + X_{min})/2)}{(X_{max} - X_{min})/2} \tag{10}$$

Minitab program is used for regression modeling and significance tests. The mathematical models for the uncoded factor levels are given in Eqs. (11) and (15). **Table 5** shows the R^2 statistics associated with the regression models.

	Y_1	Y_2	Y_3	Y_4	Y_5
R² (%)	99.35	99.57	100	99.25	99.39
R² (prediction) (%)	88.24	93.14	99.7	85.07	89.32
R² (adjusted) (%)	97.88	98.59	99.99	97.57	98.03

Table 5.
Summary of coefficient of determination values.

$$\hat{Y}_1 = 81.0151784520298 + 0.0227200449501287X_1 + 0.090808386009271X_2$$
$$+ 34.4411803062228X_3 - 0.0526452802359875X_1^2 - 0.00195145280235988X_2^2$$
$$- 18.6931720747296X_3^2 + 0.000938938053097341X_1X_2$$
$$+ 0.513403216743922X_1X_3 - 0.0987609565950274X_2X_3$$

$$(11)$$

$$\hat{Y}_2 = 10.0924651495997 + 0.00532434330664408X_1 - 0.00804942407641527X_2$$
$$- 3.24443902233461X_3 + 0.00413938053097343X_1^2 + 0.000178893805309734X_2^2$$
$$+ 1.77530383480827X_3^2 - 0.0000876106194690151X_1X_2$$
$$- 0.0481433487849417X_1X_3 + 0.00866354122770053X_2X_3$$

$$(12)$$

$$\hat{Y}_3 = 0.717642281219273 + 0.0998102261553588X_1 + 0.000230039331366765X_2$$
$$+ 0.0165307767944939X_3 - 0.00900958702064896X_1^2 - 0.0000025959X_2^2$$
$$- 0.0168692232055067X_3^2 + 0.0000584070796460183X_1X_2$$
$$+ 0.00464847590953787X_1X_3 - 0.000464847590953787X_2X_3$$

$$(13)$$

$$\hat{Y}_4 = 22.825129006883 - 0.0399906588003885X_1 - 0.112362143559489X_2$$
$$-33.6265606686333X_3 + 0.0581474926253684X_1^2 + 0.00201897492625369X_2^2$$
$$+17.8853726647001X_3^2 + 0.00091681415929201X_1X_2 - 0.603758603736482X_1X_3$$
$$+0.121209193706982X_2X_3$$

$$(14)$$

$$\hat{Y}_5 = 2449.75496212952 - 0.949312895068736X_1 - 11.2799654586319X_2$$
$$- 4567.06018645878X_3 + 6.74597935103238X_1^2 + 0.257072293510325X_2^2$$
$$+ 2496.87546116028X_3^2 - 0.130220353982304X_1X_2 - 67.5995269700804X_1X_3$$
$$+ 12.0458653954207X_2X_3$$

$$(15)$$

The R^2 values presented in **Table 5** are very close to 100%—which means the selected design parameters (magnet thickness, offset, embrace) are sufficient to mathematically model the responses. ANOVA is used to determine the model's significance. For this purpose, P-value approach is used. The summary for the ANOVA results is presented in **Table 6**.

	Y_1	Y_2	Y_3	Y_4	Y_5
P-Value	0.001	0.000	0.000	0.001	0.000
Test	<0.05	<0.05	<0.05	<0.05	<0.05
Result	Significant	Significant	Significant	Significant	Significant

Table 6.
Summary of ANOVA results.

ANOVA results presented in **Table 6** indicate that all the calculated p-values are less than α = 0.05 (5%)—which means each mathematical model is significant and can be used in optimization phase. The RSM face-centered design looks to accurately reflect the supplied set of alternator design parameters. **Table 7** displays the prediction performances of the mathematical models. $\hat{Y}_i$ is the Minitab predictions (expected values) while Y_i is the simulation results obtained from Maxwell (observed values). The prediction error percentage is denoted by PE(%) and computed using Eq. (16):

$$PE_i(\%) = \frac{|Y_i - \hat{Y}_i|}{\hat{Y}_i} 100 \tag{16}$$

Results provided in **Table 7** show that the regression models good fit the observed values and the PE(%) is quite low. Also the confirmation tests are performed for the mathematical models. For this purpose a new dataset that is composed of five new Maxwell simulation results—which is not used in the mathematical modeling phase previously—is used. Confirmations are presented in **Table 8**.

According to the confirmation results indicated in **Table 8**, the overall PE(%) is acceptable. The comparisons shown in **Tables 7** and **8** indicate that these numerical models can be used for optimization.

In the optimization phase, four different optimization methods (RSM, GA, PSO, and MSGO) from four different classes are tested for calculating the optimum design parameters. To establish the optimum factor levels, the optimization

Run (i)	Efficiency (%)			Rated torque (N.m)			Air-gap flux density (Tesla)			Armature current density (A/mm²)			Armature thermal load (A²/mm³)		
	Y_{i1}	$\hat{Y}_{i1}$	PE_{i1} (%)	Y_{i2}	$\hat{Y}_{i2}$	PE_{i2} (%)	Y_{i3}	$\hat{Y}_{i3}$	PE_{i3} (%)	Y_{i4}	$\hat{Y}_{i4}$	PE_{i4} (%)	Y_{i5}	$\hat{Y}_{i5}$	PE_{i5} (%)
1	94.08	93.911	0.18	8.88	8.893	0.15	0.89	0.890	0.01	9.86	10.032	1.71	726.16	747.929	2.91
2	93.36	93.344	0.02	8.95	8.951	0.01	1.01	1.010	0.02	10.50	10.525	0.24	822.86	824.805	0.24
3	92.58	92.521	0.06	9.02	9.024	0.04	0.89	0.890	0.04	11.17	11.265	0.85	931.11	938.546	0.79
4	92.21	92.104	0.12	9.06	9.067	0.08	1.02	1.020	0.01	11.80	11.905	0.89	982.58	994.586	1.21
5	97.54	97.625	0.09	8.56	8.554	0.07	0.89	0.890	0.02	6.11	6.029	1.34	278.45	269.456	3.34
6	98.02	98.085	0.07	8.52	8.515	0.05	1.02	1.020	0.03	5.42	5.315	1.98	219.37	211.132	3.90
7	94.69	94.870	0.19	8.82	8.805	0.17	1.02	1.020	0.02	9.30	9.119	1.98	645.47	621.831	3.80
8	96.61	96.754	0.15	8.64	8.629	0.13	0.89	0.890	0.05	7.28	7.093	2.63	396.00	375.788	5.38
9	97.00	96.878	0.13	8.61	8.622	0.14	1.02	1.020	0.00	6.78	6.936	2.24	343.20	361.126	4.96
10	97.46	97.496	0.04	8.57	8.567	0.04	0.99	0.990	0.00	6.22	6.209	0.18	288.41	281.927	2.30
11	95.01	94.996	0.01	8.79	8.794	0.05	0.99	0.990	0.05	8.99	8.970	0.22	602.48	606.677	0.69
12	93.61	93.961	0.37	8.92	8.896	0.28	0.99	0.990	0.03	10.29	9.892	4.02	789.81	746.654	5.78
13	97.53	97.201	0.34	8.57	8.595	0.29	0.99	0.990	0.01	6.13	6.497	5.65	280.17	321.040	12.73
14	97.07	97.026	0.04	8.61	8.609	0.01	0.99	0.991	0.08	6.72	6.782	0.91	336.90	341.473	1.34

Table 7.
Regression model performances.

Run (i)	Efficiency (%)			Rated torque (N.m)			Air-gap flux density (Tesla)			Armature current density (A/mm^2)			Armature thermal load (A^2/mm^3)		
	Y_{i1}	$\hat{Y}_{i1}$	PE_{i1} (%)	Y_{i2}	$\hat{Y}_{i2}$	PE_{i2} (%)	Y_{i3}	$\hat{Y}_{i3}$	PE_{i3} (%)	Y_{i4}	$\hat{Y}_{i4}$	PE_{i4} (%)	Y_{i5}	$\hat{Y}_{i5}$	PE_{i5} (%)
15	96.75	96.237	0.53	8.63	8.679	0.57	0.96	0.947	1.37	7.11	7.623	6.73	377.61	443.702	14.90
16	95.33	95.455	0.13	8.76	8.756	0.05	1.01	1.011	0.14	8.67	8.382	3.44	560.40	548.170	2.23
17	97.73	97.850	0.12	8.55	8.535	0.18	1.01	1.014	0.43	5.84	5.800	0.69	254.69	236.384	7.74
18	94.82	94.619	0.21	8.81	8.833	0.26	1.01	1.014	0.41	9.18	9.296	1.25	628.25	659.757	4.78
19	96.89	96.421	0.49	8.62	8.664	0.51	1.01	1.014	0.43	6.95	7.442	6.61	360.79	420.246	14.15

Table 8.
Confirmation tests.

algorithms will be run through these five regression models. RSM is a gradient-based method, while GA (evolutionary-based algorithm), PSO (swarm intelligence-based algorithm), and MSGO (human-based algorithm) are meta-heuristic optimization methods [24]. In this study, the performance of the multiobjective optimization using meta-heuristics is done by combining all the responses in one objective function independent from their units. To do this, the response functions must be recalculated by using the coded factor levels (instead of original levels) between -1 (for minimum value for the factor level) and $+1$ (for maximum value for the factor level). The regression models calculated from coded factor levels are given in Eqs. (17)–(21):

$$
\begin{aligned}
\hat{Y}_{1,coded} =\ & 96.7492070304818 + 0.0107779533642339X_1 - 1.15129382638011X_2 \\
& + 1.61995398230089X_3 - 0.210581120943952X_1^2 - 0.780581120943952X_2^2 \\
& - 1.1683232546706X_3^2 + 0.0375575221238924X_1X_2 \\
& + 0.25670160837196X_1X_3 - 0.493804782975135X_2X_3
\end{aligned}
$$

$$ (17) $$

$$
\begin{aligned}
\hat{Y}_{2,coded} =\ & 8.63435501474926 + 0.0011593271526898X_1 + 0.105070831577469X_2 \\
& - 0.150196460176991X_3 + 0.0165575221238939X_1^2 \\
& + 0.0715575221238936X_2^2 + 0.110956489675516X_3^2 \\
& - 0.00350442477876052X_1X_2 - 0.0240716743924708X_1X_3 \\
& + 0.0433177061385025X_2X_3
\end{aligned}
$$

$$ (18) $$

$$
\begin{aligned}
\hat{Y}_{3,coded} =\ & 0.990846656833825 + 0.0647760570304818X_1 \\
& + 0.000223942969518185X_2 + 0.000130973451327435X_3 \\
& - 0.0360383480825959X_1^2 - 0.00103834808259587X_2^2 \\
& - 0.00105432645034415X_3^2 + 0.00233628318584071X_1X_2 \\
& + 0.0232423795476892X_1X_3 - 0.00232423795476893X_2X_3
\end{aligned}
$$

$$ (19) $$

$$\hat{Y}_{4,coded} = 7.07668220255654 - 0.0185867748279251X_1 + 1.25942010816126X_2$$
$$- 1.69733805309735X_3 + 0.232589970501475X_1^2 + 0.807589970501475X_2^2$$
$$+ 1.11783579154375X_3^2 + 0.0366725663716815X_1X_2$$
$$- 0.30187930186824X_1X_3 + 0.606045968534907X_2X_3$$

$$(20)$$

$$\hat{Y}_{5,coded} = 377.792067158309 - 0.571060788032038X_1 + 150.328878248349X_2$$
$$- 212.806948672566X_3 + 26.9839174041298X_1^2 + 102.82891740413X_2^2$$
$$+ 156.054716322517X_3^2 - 5.20881415929203X_1X_2$$
$$- 33.7997634850401X_1X_3 + 60.2293269771036X_2X_3$$

$$(21)$$

The objective function is given in Eq. (22) and Eq. (23). The aim is to maximize the efficiency (Y_1), while holding the air-gap flux density (Y_3) at 1 Tesla and minimizing the rest of the responses (Y_2, Y_4, Y_5).

$$Z = |(Y_{1,coded}/max(Y_{i1}))| - |(Y_{2,coded}/max(Y_{i2}))| \qquad (22)$$
$$- |(Y_{3,target}/max(Y_{i3})) - (Y_{3,coded}/max(Y_{i3}))| - |(Y_{4,coded}/max(Y_{i4}))|$$
$$- |(Y_{5,coded}/max(Y_{i5}))|$$

Min Z s.t. X1 $\in[-1,1]$; X2$\in[-1,1]$; X3$\in[-1,1]$

Note that the $Y_{3,target} = 1$ Tesla in the equation of Z. In addition; $max(Y_{i1})$, $max(Y_{i2})$, $max(Y_{i3})$, $max(Y_{i4})$, and $max(Y_{i5})$ are the maximum observed response values presented in **Table 4** (which are 98.02, 9.06, 1.02, 11.8, and 982.58 for this problem, respectively). If the readers would like to use the Matlab codes referred in the reference [28] for MSGO, note that the signs of the each term are the exact opposite (since the codes in the reference are coded according to maximization problems). Then the *Z* function set in the Matlab code is given in Eq. (24):

$$Z = -|(Y_{1,coded}/98.02)| + |(Y_{2,coded}/9.06)| + |(1/1.02) - (Y_{3,coded}/1.02)| + |(Y_{4,coded}/11.8)|$$
$$+ |(Y_{5,coded}/982.58)|$$

$$(24)$$

MSGO, PSO, GA, and RSM are run through these mathematical models to perform multi-objective optimization. **Table 9** summarizes the optimized factor levels and the calculated CPU times (at a PC: Intel i5 4GB RAM), for each method. In this table, *nPop* and *MaxIt* represent the population size and maximum number of iterations, respectively. For MSGO, c and SAP are set as 0.2 and 0.7, respectively. In PSO, the parameters of the algorithm are set as: w = 1, w_{damp} = 0.99, c_1 = 1.5, c_2 = 2.0. In the GA, we use the crossover rate = 0.50 and the mutation rate = 0.20. The optimization results for these optimization methods are presented in **Table 10**.

Results presented in **Table 10** indicate that the meta-heuristics superiors RSM with a quite bit difference. When compared among themselves, MSGO and PSO together give better results than GA. The MSGO and PSO give the same optimization results. So

Method	Run parameters		Coded factor levels			Uncoded factor levels			CPU time
	nPop	*MaxIt*	X_1	X_2	X_3	X_1	X_2	X_3	
MSGO	30	2000	**0.7396**	**-1**	**1**	**5.48**	**0**	**1**	5
PSO	100	1000	**0.7396**	**-1**	**1**	**5.48**	**0**	**1**	7
RSM	N/A	N/A	0.2	−0.5	1	4.4	10	1	N/A
GA	8	100,000	0.1528	−1	0.9485	4.31	0	0.99	9

Table 9.
Optimized factor levels for each method.

	$\hat{Y}_1$	$\hat{Y}_2$	$\hat{Y}_3$	$\hat{Y}_4$	$\hat{Y}_5$
Target:	Max	Min	1 Tesla	Min	Min
MSGO	**98.1202**	**8.513**	1.0192	**5.3024**	**206.5071**
PSO	**98.1202**	**8.513**	1.0192	**5.3024**	**206.5071**
RSM	97.8696	8.5352	1.0025	5.7079	236.194
GA	98.0959	8.5157	**1.0002**	5.3895	209.4387

Table 10.
Summary of the optimization results.

the optimized factor levels of MSGO and also same as PSO are used for designing the optimized design. The optimum factor levels are calculated as: magnet thickness: 5.48 mm, offset: 0 mm, embrace: 1%. However, confirmation results of these four methods are given together in **Table 11**. The observed responses and the fitted responses are presented in **Table 11**. Also the PE (%) values are calculated for each response in terms of the methods.

The optimized PMSG's magnetic flux distribution and the voltage graphs are presented in **Figures 7** and **8**, respectively. The graphs for flux linkage, power, and torque are given in **Figure 9**, **Figure 10**, and **Figure 11**, respectively.

In order to obtain the desired responses, the embrace must be maximum. Also the magnet thickness must be bigger than 4 mm. For this sample PMSG structure in the article, the results showed that offset has no discernible effect on responses (causes little changes).

As previously stated, this issue is only relevant to the PMSG in this case study. Additional optimization methods can be used to expand on these findings and discussions such as bat algorithm (BA) [29], grew wolf optimizer (GWO) [30], whale

Method	Y_{i1}	$\hat{Y}_{i1}$	PE_{i1} (%)	Y_{i2}	$\hat{Y}_{i2}$	PE_{i2} (%)	Y_{i3}	$\hat{Y}_{i3}$	PE_{i3} (%)	Y_{i4}	$\hat{Y}_{i4}$	PE_{i4} (%)	Y_{i5}	$\hat{Y}_{i5}$	PE_{i5} (%)
MSGO	**98.03**	**98.1202**	0.09	**8.52**	**8.513**	0.08	1.01	1.0192	0.90	**5.4**	**5.3024**	1.84	**217.9**	**206.5071**	5.52
PSO	**98.03**	**98.1202**	0.09	**8.52**	**8.513**	0.08	1.01	1.0192	0.90	**5.4**	**5.3024**	1.84	**217.9**	**206.5071**	5.52
RSM	97.84	97.8696	0.03	8.54	8.5352	0.06	**1**	**1.0025**	0.25	5.69	5.7079	0.31	241.3	236.194	2.16
GA	98.01	98.0959	0.09	**8.52**	8.5157	0.05	**1**	**1.0002**	0.02	5.42	5.3895	0.57	219.76	209.4387	4.93

Table 11.
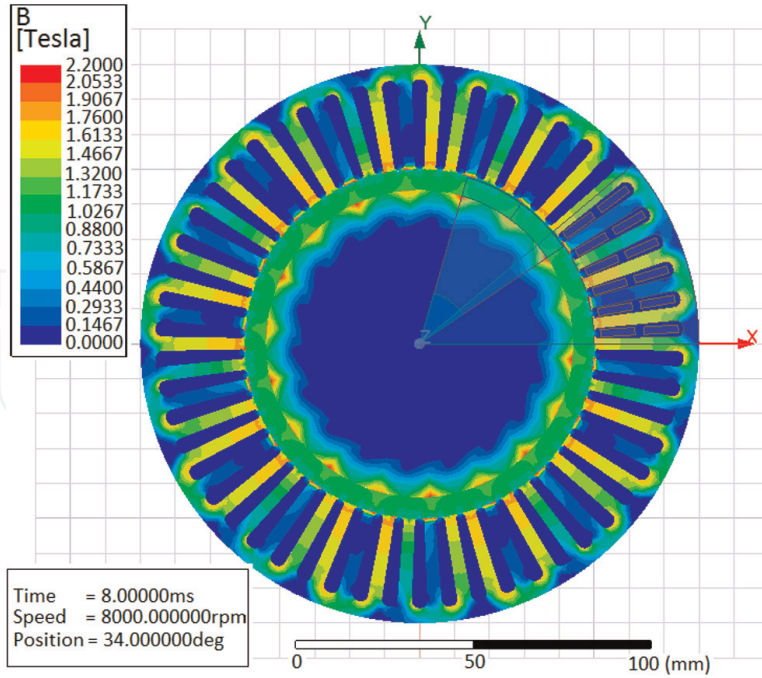*Confirmations for the optimized factor levels.*

Figure 7.
Magnetic flux density distribution of the optimized PMSG.
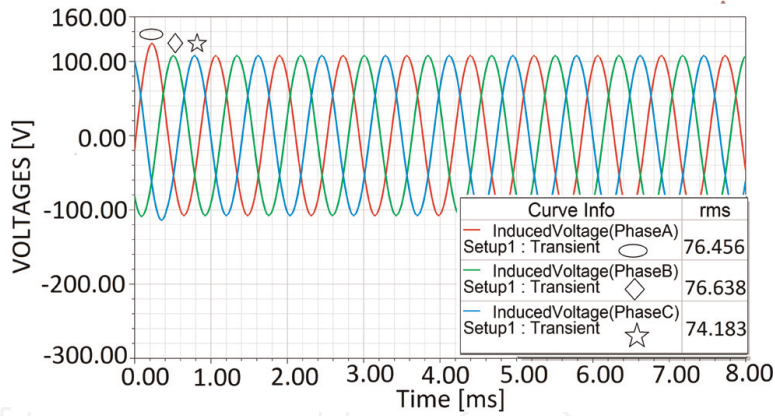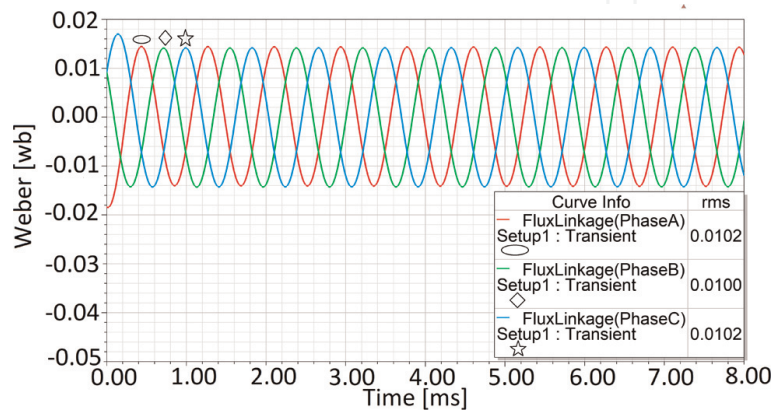

Figure 8.
Voltage graph of the optimized PMSG.

Figure 9.
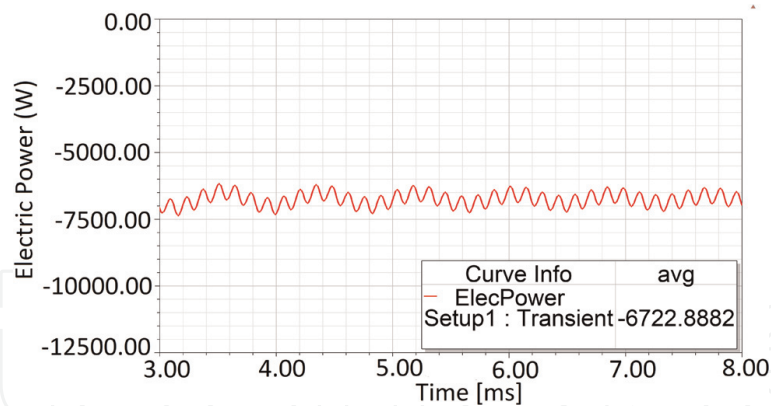*Flux linkage of the optimized PMSG.*

Figure 10.
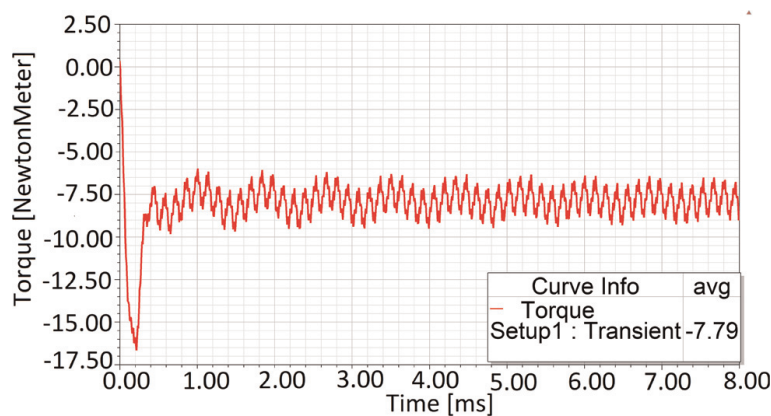*Power graph of the optimized PMSG.*

Figure 11.
Torque graph of the optimized PMSG.

optimization (WOA) [31], grasshopper optimization algorithm (GOA) [32] etc., in the future research studies.

4. Conclusion

The design of an 18-poled 8000 rpm 7 kVA PMSG is optimized in this study. The goal is to determine the optimal levels of magnet thickness (MH), offset, and embrace (EMB) to keep the air-gap flux density at 1 tesla while maximizing efficiency and minimizing other responses. For this purpose, Ansys Maxwell is used for calculating the responses and Minitab is used for mathematically modeling the relations between the factors and the responses by using simulation results. Then MSGO, PSO, RSM, and GA are used for optimization by running these algorithms through the regression models. Matlab coding is performed for this stage. Although the results of the four methods are nearly identical, MSGO and PSO outperform the other methods for the sample PMSG presented in this study. Although the results of the four methods are nearly identical, one advantage of RSM is that it does not require program coding and allows for visual examination of the relationships between factors and responses. The RSM is clearly less complex than the PSO, MSGO, and GA, according to the time complexity analysis. When comparing the PSO, MSGO, and GA, it is clear that the MSGO has fewer parameters to tune and produces extremely accurate results, making it extremely efficient. In the future, we plan to expand the work to include additional

design parameters, higher power groups, and additional optimization methods. The optimum factor levels are calculated as: magnet thickness: 5.48 mm, offset: 0 mm, embrace: 1% at the end of optimization phase. The embrace must be at its peak in order to obtain the desired responses. In addition, the magnet thickness must be greater than 4 mm. The results demonstrated that offset has no discernible effect on the selected responses for the selected PMSG structure in this manuscript.

Acknowledgements

Conflict of interest

"The authors declare no conflict of interest."

Author details

Aslan Deniz Karaoglan[1*], Deniz Perin[2] and Kemal Yilmaz[2]

1 Department of Industrial Engineering, Balikesir University, Balikesir, Turkey

2 Department of R&D, ISBIR Electric Company, Balikesir, Turkey

*Address all correspondence to: deniz@balikesir.edu.tr

IntechOpen

References

[1] Gizolme O, Thollon F, Clerc G, Rojat G. Shape optimization of synchronous machine rotor. International Journal of Applied Electromagnetics and Mechanics. 1998;**9**: 263-275

[2] Gillon F, Brochet P. Screening and response surface method applied to the numerical optimization of electromagnetic devices. IEEE Transactions on Magnetics. 2000;**36**: 1163-1167

[3] Jolly L, Jabbar MA, Qinghua L. Design optimization of permanent magnet motors using response surface methodology and genetic algorithms. IEEE Transactions on Magnetics. 2005; **41**:3928-3930

[4] Fang L, Jung JW, Hong JP, Lee JH. Study on high-efficiency performance in interior permanent-magnet synchronous motor with double-layer PM design. IEEE Transactions on Magnetics. 2008; **44**:4393-4396

[5] Hasanien HM, Muyeen SM. A Taguchi approach for optimum design of proportional-integral controllers in cascaded control scheme. IEEE Transaction on Power Systems. 2013;**28**: 1636-1644

[6] Zhang CJ, Chen ZH, Mei QX, Duan JJ. Application of particle swarm optimization combined with response surface methodology to transverse flux permanent magnet motor optimization. IEEE Transactions on Magnetics. 2017; **53**:8113107

[7] Chai W, Lipo TA, Kwon BI. Design and optimization of a novel wound field synchronous machine for torque performance enhancement. Energies. 2018;**11**:2111

[8] Islam MJ, Moghaddam RR. Loss reduction in a salient pole synchronous machine due to magnetic slot wedge and semi-closed stator slots. In: 13th International Conference on Electrical Machines (ICEM), 03–06 Sept. 2018. Alexandroupoli, Greece: IEEE; 2018. pp. 1267-1272

[9] Soleimani J, Ejlali A, Moradkhani M. Transverse flux permanent magnet generator design and optimization using response surface methodology applied in direct drive variable speed wind turbine system. Periodicals of Engineering and Natural Sciences. 2019;**7**:36-53

[10] Karaoglan AD, Perin D, Yilmaz K. Multiobjective design optimization of stator for synchronous generator using bat algorithm and analysis of magnetic flux density distribution. Electric Power Components and Systems. 2021;**49**: 919-929. DOI: 10.1080/ 15325008.2022.2049651

[11] Karaoglan AD, Perin D. Design optimization of a 4-poled 1500 rpm 25 kVA SG to obtain the desired magnetic flux density distributions by using RSM. Journal of Scientific & Industrial Research. 2022;**81**:84-93

[12] Sadeghierad M, Amini S, Ziaie S. Comparison of alternative configurations for a high speed alternator for microturbines. In: 21th International Power Systems Conference, 13–15 Nov. 2006. Tehran, Iran: PSC2006; 2006. pp. 587-595

[13] Sadeghierad M, Darabi A, Lesani H, Monsef H. Optimal design of the generator of microturbine using genetic algorithm and PSO. International Journal of Electrical Power & Energy Systems. 2010;**32**:804-808

[14] Ismagilov FR, Vavilov VE, Gusakov DV, Ou J. High-speed generator with tooth-coil winding, permanent magnets and new design of a stator magnetic core made from amorphous alloy. In: 25th International Workshop on Electric Drives-Optimization in Control of Electric Drives (IWED); 31 January-02 February 2018. Moscow, Russia: IEEE; 2018

[15] Guo J, Jin YM, Zhang Y, Xue MZ, Luan Y. Optimization design of high-speed generator for micro turbojet engine based on GDSFD-AL method. In: IEEE Transportation Electrification Conference and Expo, Asia-Pacific (ITEC); 08–10 May 2019. Seogwipo-si, South Korea: IEEE; 2019. pp. 144-150

[16] Montgomery DC. In: Haboken NJ, editor. Design and Analysis of Experiments. New Jersey, USA: John Wiley & Sons; 2013

[17] Mason RL, Gunst RF, Hess JL. Statistical Design and Analysis of Experiments. Haboken, NJ: John Wiley & Sons; 2003

[18] Karaoglan AD. Optimizing plastic extrusion process via grey wolf optimizer algorithm and regression analysis. Journal of Scientific & Industrial Research. 2021;**80**:34-41

[19] Holland JH. Adaptation in Natural and Artificial Systems. Cambridge, UK: MIT Press; 1975

[20] Goldberg DE. Genetic Algorithms in Search, Optimization and Machine Learning. Boston, MA: Addison-Wesley Longman Publishing Co. Inc; 1989

[21] Haupt R, Haupt SE. Practical Genetic Algorithms. Habokenm NJ: John Wiley & Sons; 2004

[22] Kennedy J, Eberhart R. Particle swarm optimization. In: IEEE International Conference on Neural Networks; 27 November – 1 December 1995. Perth, Western Australia: IEEE; 1995. pp. 1942-1948

[23] Wei Y, Qiqiang L. Survey on particle swarm optimization algorithm. Engineering Science. 2004;**5**: 87-94

[24] Lalwani S, Sharma H, Satapathy SC, Deep K, Bansal JC. A survey on parallel particle swarm optimization algorithms. Arabian Journal for Science and Engineering. 2019;**44**:2899-2923

[25] Dai H-P, Chen D-D, Zheng Z-S. Effects of random values for particle swarm optimization algorithm. Algorithms. 2018;**11**:23

[26] Naik A, Satapathy SC, Abraham A. Modified social group optimization—A meta-heuristic algorithm to solve short-term hydrothermal scheduling. Applied Soft Computing. 2020;**95**:106524

[27] Satapathy S, Naik A. Social group optimization (SGO): A new population evolutionary optimization technique. Complex & Intelligent Systems. 2016;**2**: 173-203

[28] Naik A. Modified Social Group Optimization algorithm [Internet]. 2021. Available from: https://www.math works.com/matlabcentral/fileexchange/ 78272-modified-social-group-optimiza tion-algorithm [Accessed: January 29, 2021], MATLAB Central File Exchange.

[29] Yang XS. A New Metaheuristic Bat-Inspired Algorithm. Nature Inspired Cooperative Strategies for Optimization (NISCO 2010). Studies in Computational Intelligence. Berlin: Springer; 2010. pp. 65-74

[30] Mirjalili S, Mirjalili SM, Lewis A. Grey wolf optimizer. Advances in Engineering Software. 2014;**69**:46-61

[31] Mirjalili S, Lewis A. The whale optimization algorithm. Advances in Engineering Software. 2016;**95**:51-67

[32] Saremi S, Mirjalili S, Lewis A. Grasshopper optimisation algorithm: Theory and application. Advances in Engineering Software. 2017;**105**:30-47